PCCP

PAPER

View Article Online
View Journal | View Issue

Cite this: *Phys. Chem. Chem. Phys.*, 2014, **16**, 19258

Controlled amino-functionalization by electrochemical reduction of bromo and nitro azobenzene layers bound to Si(111) surfaces†

Daniela Ullien,[a] Peter C. Thüne,‡[b] Wolter F. Jager,[a] Ernst J. R. Sudhölter[a] and Louis C. P. M. de Smet*[a]

Received 4th June 2014,
Accepted 17th July 2014

DOI: 10.1039/c4cp02464h

www.rsc.org/pccp

4-Nitrobenzenediazonium (4-NBD) and 4-bromobenzenediazonium (4-BBD) salts were grafted electrochemically onto H-terminated, p-doped silicon (Si) surfaces. Atomic force microscopy (AFM) and ellipsometry experiments clearly showed layer thicknesses of 2–7 nm, which indicate multilayer formation. Decreasing the diazonium salt concentration and the reaction time resulted in a smaller layer thickness, but did not prevent the formation of multilayers. It was demonstrated, mainly by X-ray photoelectron spectroscopy (XPS), that the diazonium salts not only react with the H-terminated Si surface, but also with electrografted phenyl groups *via* azo-bond formation. These azo bonds can be electrochemically reduced at E_{red} = −1.5 V, leading to the corresponding amino groups. This reduction resulted in a modest decrease in layer thickness, and did not yield monolayers. This indicates that other coupling reactions, notably a biphenyl coupling, induced by electrochemically produced phenyl radicals, take place as well. In addition to the azo functionalities, the nitro functionalities in electrografted layers of 4-NBD were independently reduced to amino functionalities at a lower potential (E_{red} = −2.1 V). The presence of amino functionalities on fully reduced layers, both from 4-NBD- and 4-BBD-modified Si, was shown by the presence of fluorine after reaction with trifluoroacetic anhydride (TFAA). This study shows that the electrochemical reduction of azo bonds generates amino functionalities on layers produced by electrografting of aryldiazonium derivatives. In this way multifunctional layers can be formed by employing functional aryldiazonium salts, which is believed to be very practical in the fabrication of sensor platforms, including those made of multi-array silicon nanowires.

1 Introduction

Proteins, antigens and DNA are the main target molecules for biosensors. An important aspect in achieving selectivity of such sensors is the attachment of the appropriate receptor molecules to the sensing layer. Depending on the field of application and the type of sensor platform this may require chemical attachment. Amide bond formation is one of the most important strategies among different approaches for the chemical immobilization of receptors like antibodies or complementary DNA.[1] For example, receptors carrying a carboxylic acid group can be chemically attached to an amino-functionalized (sensor) surface *via* carbodiimide chemistry.[2]

Silicon-based electronic devices have found increasing importance in sensor development since they can be built reproducibly at large scales and at low cost, using standard semiconductor technologies. Moreover, by making use of different doping levels one can tune the semiconducting behavior of silicon. For example, silicon nanowire-based, field-effect transistors (SiNW FETs) have shown a rapid, label-free, sensitive detection of biological and chemical species.[3,4] The surface modification strategies that have been explored on Si include silanization and hydrosilylation on oxide or H-terminated Si surfaces, respectively.[5,6] In this latter reaction, 1-alkenes or 1-alkynes react with Si–H groups at the surface to form Si–C bonds, which are more stable than the Si–O bonds on silicon oxide surfaces as these are susceptible towards hydrolysis and are thermally labile.[7] In addition, in the case of Si–C bond formation true monolayers are formed, and the sensing event (target–analyte interaction) takes place closer to the conducting surface, which increases the sensitivity of the device.[5]

[a] *Department of Chemical Engineering, Delft University of Technology, Julianalaan 136, 2628 BL Delft, The Netherlands. E-mail: l.c.p.m.desmet@tudelft.nl; Fax: +31 152788668; Tel: +31 152782636*
[b] *Faculty of Chemical Engineering, Catalysis & Energy, Eindhoven University of Technology, 5600 MB Eindhoven, The Netherlands*

† Electronic supplementary information (ESI) available. See DOI: 10.1039/c4cp02464h

‡ Current address: Fontys Hogescholen, Rachelsmolen 1, 5612 MA Eindhoven, The Netherlands.

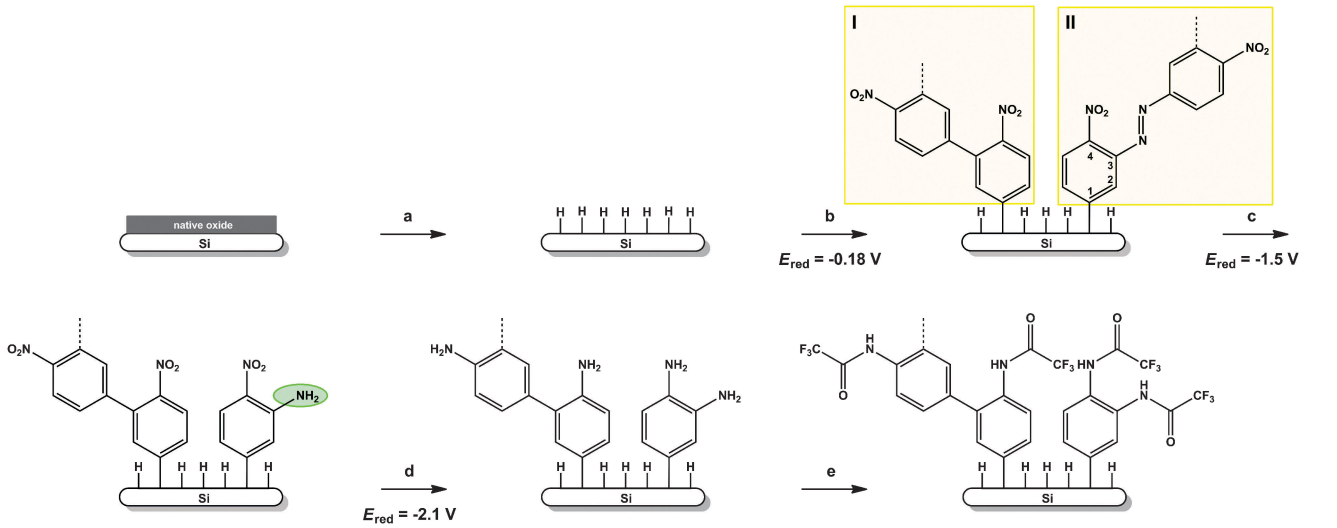

Scheme 1 Schematic representation of the surface etching of Si(111) (step a) and the electrografting of 4-NBD onto the H-terminated Si surface (step b), forming biphenyl-coupled (box I) and azo-coupled products (box II). The dashed lines indicate the further growth of the layers, both *via* biphenyl coupling and the formation of azo bonds. For matter of clarity, only one example of each coupling is drawn, but the attached structures can also be branched and contain both types of coupling. Next, a two-step electroreduction yields amino groups from the azo-bond (oval; step c) and from the nitro groups (step d). The formed amino groups are modified with TFAA, which results in amide formation (step e). The reported voltages represent the minimal voltages applied during the electrografting (step a) and the electroreduction (steps c and d). All values reported are relative to the standard calomel electrode (SCE).

An interesting alternative to the hydrosilylation of 1-alkenes and 1-alkynes on the H-terminated Si surface is the electrografting of aryl diazonium salts onto these surfaces. In this reaction—which has been reported on carbon and metal surfaces as well—the diazonium salt is reduced *via* the uptake of an electron from the surface upon which N_2 is released. Subsequently, two resulting aryl radicals react with the surface, the first to abstract a hydrogen atom and the second to react with the thus formed surface radical, to form a stable Si–C bond.[8] Very recently, diazonium chemistry has been employed to graft antibodies targeted against a prostate cancer risk biomarker onto SiNW surfaces, resulting in resistor-mode biosensors.[9] In contrast to silanization and hydrosilylation, the diazonium electrochemical reaction allows one to attach organic molecules to specific areas of a surface. For example, adjacent wires that are part of multi-array devices can be modified with different functionalities by addressing individual nanowires electrochemically. Very recently, a novel method for the selective surface modification of SiNWs with metal particles by nanoscale Joule heating was demonstrated.[10] With light-initiated hydrosilylation,[11] in combination with masking techniques also patterns can be made, but this templating cannot be performed at nm-level resolution.

Electrochemical grafting of diazonium salts onto carbon materials,[12] metals[13] or semiconductors[14] has been known for more than 20 years.[15] 4-Nitrobenzenediazonium (4-NBD) was electrografted for the first time onto oxide-free silicon surfaces by de Villeneuve in 1997.[14] Later, this type of functionalization was used to obtain aminobenzene-terminated Si surfaces *via* the chemical reduction of the nitro groups, enabling the chemical attachment of amine-terminated, single-stranded DNA *via* glutaraldehyde coupling, making the surface ready for hybridization experiments.[16]

The electrografting of diazonium salts onto carbon, metal and semiconductor electrodes leads to the formation of layers that are thicker than one monolayer.[15,17,18] Biphenyl coupling and the formation of azo bonds are common side reactions that have been demonstrated on Si(111) surfaces, metals and C-electrodes.[19] X-Ray photoelectron spectroscopy (XPS) studies of the N_{1s} emission clearly indicate the presence of azo bonds,[19,20] which point to the formation of phenyldiazene ('azo') structures. Recently, the electrochemical reduction of azo bonds to amines was demonstrated for electrografted layers on gold.[21]

Herein we describe the electrografting of 4-bromobenzenediazonium (4-BBD) and 4-NBD onto H-terminated Si(111) surfaces and the independent electrochemical reduction of azo bonds that are present in these layers (Schemes 1 and 2). This methodology enables the fabrication of surfaces with amino functionalities in addition to the substituents at the 4-position of the benzenediazonium compound that was grafted onto the surface. We demonstrated the utility of the electrochemically generated amino functionalities by the reaction with trifluoroacetic anhydride.

2 Experimental section

2.1 Materials and reagents

4-Nitro and 4-bromobenzenediazonium tetrafluoroborate, sulfuric acid, and acetonitrile (ACN, HPLC grade, $\geq$99.9%) were purchased from Sigma-Aldrich. Ammonium fluoride, tetrabutylammonium tetrafluoroborate ($(Bu_4N)BF_4$) and trifluoroacetic

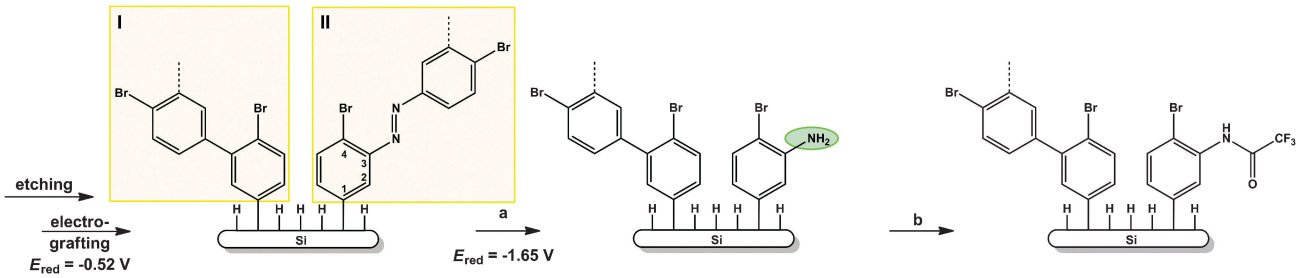

Scheme 2 Schematic representation of the electrochemical reduction of 4-BBD-modified Si(111) surfaces (step a), followed by the functionalization of the resulting amino groups (step b). Boxes I and II represent the biphenyl and azo-coupled products, respectively. The oval highlights the amino functionality obtained from the electrochemical reduction of the azo bond. All values reported are relative to the standard calomel electrode (SCE).

anhydride (TFAA) were purchased from Fluka. All chemicals were used as received. All aqueous solutions were prepared in MilliQ water (resistivity $>$ 10 MΩ). Boron-doped (0.001–0.005 Ω cm^{-1}) silicon (Si) (111) wafers, with a thickness of 500–550 μm and covered with native oxide, were obtained from Siltronix.

2.2 Electrochemical equipment

All 3-electrode electrochemical reactions were performed using a CH Instruments potentiostat (model CHI600D) equipped with a picoamp booster with Faraday cage (model CHI200B). In this configuration, Si(111) samples were used as the working electrodes (WE) and mounted in a home-made Teflon cell with a Viton O-ring with an area of 0.25 cm^2. The back contact (BC) was achieved *via* scratching InGa eutectic on the back side of the Si sample. A Pt wire and a standard calomel electrode (SCE) were used as a counter electrode (CE) and reference electrode (RE), respectively.

2.3 Sample treatment

Cleaning and etching of the surface (Scheme 1, step a). Si dies of ∼1 cm × ∼1 cm were cleaned in acetone and water according to manufacturer's specifications to remove the polymer coating preventing silicon chips from contaminants, followed by drying in a stream of nitrogen. The following steps were performed after the sample was mounted in the O-ring cell (see Section 2.2). Etching was performed in 40% NH_4F (aq) for 15 minutes to prepare a H-terminated Si surface. The etching solvent was removed *via* a decanting step, which was followed by a rinsing step with MilliQ water and a drying step using a stream of nitrogen.

Electrografting (Scheme 1, step b). A solution of 2.5 mM of diazonium salt in 25 mM $(Bu_4N)BF_4$ in ACN was added to the cell and electrografting experiments were carried out by applying a voltage scan from 0.20 V to −0.60 V at 0.05 V s^{-1} (step b in Scheme 1). Afterwards, the samples were rinsed with ACN, ethanol, and water prior to analyses or further modification. In the experiments described in Section 3.1 three different concentrations of 4-BBD were used (0.025, 0.25 and 2.5 mM) and also different electrografting times have been used (5, 20 and 200 s). The samples described in Section 3.2 were treated as described above using 2.5 mM diazonium salt and 200 s of electrografting time. Samples modified with 4-NBD and 4-BBD without any post-treatment steps are referred to as 4-NBD- and 4-BBD-modified Si samples, respectively.

Electroreduction (Scheme 1, steps c and d; Scheme 2, step a). Further electroreduction of the resulting samples was performed in 25 mM $(Bu_4N)BF_4$ in ACN by applying a voltage scan from −0.60 to −1.5 or −2.2 V at 0.05 V s^{-1}. Subsequently, the samples were cleaned with ACN, ethanol, water and dried with a stream of dry nitrogen gas.

Reaction with TFAA (Scheme 1, step e; Scheme 2, step b). A solution of 30 μL of TFAA in 1 ml of toluene was allowed to react with the electrochemically reduced samples for 2 h at room temperature. Then the samples were washed with toluene, ethanol and water and dried with a stream of dry nitrogen gas.

2.4 XPS

The XPS measurements were carried out on a Thermo Fisher Scientific, K Alpha model, equipped with a monochromatic Al Kα X-ray source. XPS measurements were taken in normal emission with a spot size of 400 μm at a pressure of 10^{-9} mbar. During all XPS measurements the flood gun was enabled to compensate for the potential charging of surfaces. The spectra were analyzed using Avantage processing software.

2.5 Atomic force microscopy (AFM)

The AFM experiments were carried out in air using an NTEGRA AFM (NT-MDT) equipped with an NSG30 series silicon tip (resonance frequency 240–440 kHz, force constant 22–100 N m^{-1}). First, height images were collected in the tapping mode. Then the scratching mode was applied to remove the soft, grafted layers, followed by a tapping-mode measurement again. The thickness of the removed layer was determined by comparing the profile heights between scratched and unscratched areas (3 samples per modification condition).

2.6 Ellipsometry

Ellipsometry measurements were performed using an M-2000F spectroscopic ellipsometer (J. A. Woollam Co., Inc), equipped with a 75 W Xe arc light source. The experiments were performed at an incident angle of 70°. The optical thickness was determined using a standard model available in the CompleteEase software, *i.e.* Si with a transparent film on top of it. This model makes use of the optical parameters for Si as reported by Herzinger *et al.*,[22] while for the transparent film (modelled as a Cauchy film) the following values have been used: n = 1.5 and k = 0.

3 Results and discussion

3.1 Electrografting onto H-terminated Si(111)

4-NBD and 4-BBD were electrografted onto H-terminated Si(111) electrodes. Fig. 1a presents the typical Cyclic Voltammetry (CV) results. Grafting of 4-NBD and 4-BBD takes place at −0.18 V and −0.52 V *vs.* SCE, respectively (Fig. 1a, cycle i). The major contribution to the different electrografting potentials is the difference in the nature of the functional group of the diazonium salt: stronger electron withdrawing groups like nitro groups facilitate the reduction. When the samples were exposed to a subsequent second cycle under the same conditions, no electroreduction peaks were observed (Fig. 1a, cycle ii). This suggests that no electrografting of diazonium takes place after the first CV cycle, which is in line with reports from others.[14]

The electrografting of the 4-substituted benzenediazonium salts onto Si was monitored by XPS, concentrating mainly on the N_{1s} region spectra. The N_{1s} binding energies of the $[C_6H_5(N_2)]BF_4$ salt are reported to be 405.1 eV and 403.8 eV.[23] After the grafting of 4-NBD onto Si the N_{1s} region spectrum shows three contributions at ∼400 eV, ∼402 eV and ∼406 eV (Fig. 1b, blue circles). The major peak near 406 eV is attributed to the NO_2 functionality of 4-nitrobenzene grafted onto Si. The minor peak near 402 eV is assigned to the tetrabutylammonium (TBA^+) cation used in the procedure.[24] The peak near 400 eV is attributed to the azo group (–N=N–)[25] which is formed in a subsequent electrophilic aromatic substitution reaction of aryldiazonium ions with already grafted aryl moieties on the surface.[19] In the literature multiple assignments for the 400 eV peak have been given. It is mainly referred to as the 'reduced form of nitrogen', or even to the amino groups that are formed upon the reduction of the nitro group during the electrografting procedure.[14,20,26] Depending on the intensity of the X-ray source, the exposure time and likely also the photon energy, photoreduction of the nitro groups to amino groups can take place during XPS analysis.[27] We verified the N_{1s} signal under our experimental conditions and no detectable change was found (time-resolved data are provided in Fig. A1 of the ESI†). Although the XPS peak of 4-aminobenzene appears at around 400 eV, we have demonstrated that the reduction of nitro groups in ACN takes place at a more negative potential so that no amino groups are present at this stage, *vide infra*. Moreover, this peak is also present when 4-BBD is used, albeit at slightly lower binding energy (Fig. 1b, red circles, 399.5 eV). This lower electron binding energy may be due to the difference in electron withdrawing properties of Br *versus* NO_2. In the case of Br the electron-withdrawing effect is smaller, making it easier to emit N_{1s} electrons, which results in a lower binding energy.

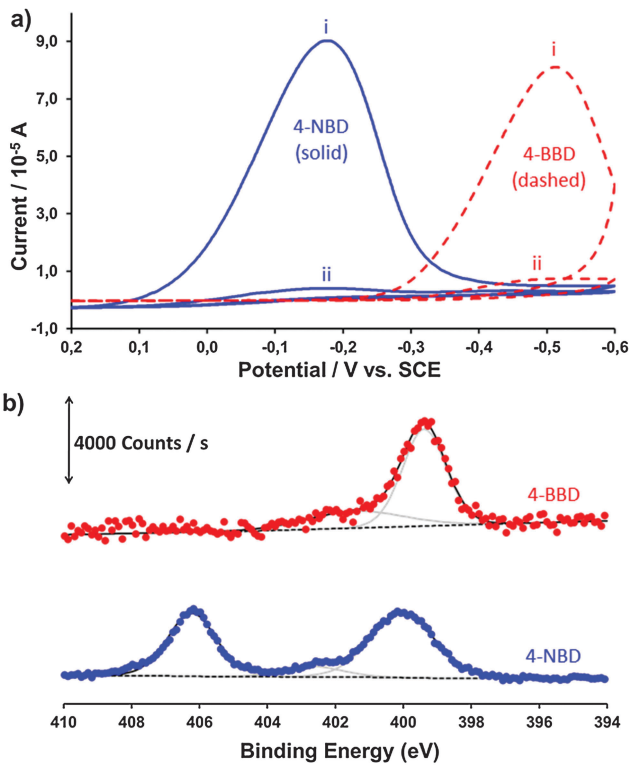

Fig. 1 (a) CV data on the electrografting of 4-NBD (blue solid) and 4-BBD (red dashed) in ACN onto H-terminated Si(111), where i and ii refer to the cycle number, and (b) XPS N_{1s} region spectra of 4-NBD- and 4-BBD modified Si(111) (blue and red, respectively). The dashed line represents the baseline, the deconvoluted peaks are given in grey solid lines and the black solid line represents the envelop.

Since the 400 eV peak indeed reflects the presence of azo bonds, the N_{1s} region spectrum of grafted 4-BBD can be used to calculate the amount of azo bonds present in the grafted layer. Typical XPS results obtained under standard electrografting conditions of 2.5 mM aryldiazonium salt and 200 s of reaction time showed 24% Si, 56% C, 5.3% Br and 1.3% N_{400}. The averaged ratio N_{400}/Br (measured for 5 samples under the same electrografting conditions) was found to be 0.24 ± 0.08, *i.e. 24 nitrogen atoms per 100 bromide atoms. Based on the structure depicted in Scheme 2, this means that on average 24% of all aryl groups present in 4-BBD-modified Si are attached via* an azo bond.

In this work we performed experiments using different diazonium salt concentrations and electrografting reaction times and analyzed the thickness of the resulting layers with ellipsometry and AFM (Fig. 2). The measurement of the layer thickness with AFM is possible by comparing the profile height of scratched *vs.* unscratched surfaces as described in Section 2.5.

The layer thickness data obtained from AFM and ellipsometry measurements correlate well. The data show that the thickness of the grafted material decreases with a decrease in the electrografting time. Under the conditions used by us we could not reduce the thickness to a sub-nanometer monolayer level, even by decreasing the concentration 100 times. Even for concentrations as low as 0.025 mM of 4-BBD, the observed layer thickness corresponds to 3 to 4 phenyl groups. The time-dependent results suggest that the grafting is not specific, *i.e.* before all possible Si–H sites are occupied, side reactions—biphenyl and azo coupling—already occur (boxes I and II in Schemes 1 and 2, respectively). In the next section we describe the results of the electroreduction of the azo bonds.

3.2 Electroreduction of grafted layers

After electrografting, the samples were immersed in ACN and exposed to a second CV cycle, during which a more negative

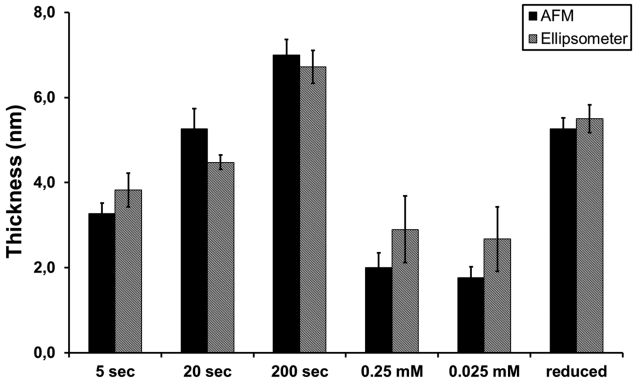

Fig. 2 Concentration- and time-dependent data on the layer thickness from ellipsometric and AFM analysis of BBD-modified Si. In the cases of 5, 20 and 200 s time of CV cycle, 2.5 mM of 4-BBD was used. In the cases of 0.25 and 0.025 mM of 4-BBD, 200 s of electrografting time was applied. The 'reduced' sample shows the thickness after electroreduction, step a in Scheme 2 of the 2.5 mM 4-BBD for 200 s of electrografting.

potential was applied down to −2.2 V (Fig. 3). The overall reduction is irreversible. In the reduction of 4-NBD grafted layers (Fig. 3, blue solid line) peaks are observed at −1.5 V and −2.1 V. In the case of 4-BBD (Fig. 3, red dashed line) one peak at −1.65 V is observed. It is proposed from these observations to attribute the peak at −1.5/−1.65 V to the reduction of the azo linkage, and the peak at −2.1 V to the reduction of the nitro substituent to an amino group. The small difference in the reduction peak of the azo bonds in the 4-nitro and 4-bromo substituted molecules can be understood from the higher electron affinity originating from the nitro group. The thickness of the grafted layers has decreased after the reduction (Fig. 2). For example, with AFM we measured the average thickness of grafted layers of 7.0 ± 0.4 nm, and after the electroreduction the average layer thickness was 5.3 ± 0.3 nm, *i.e.* a reduction of 25%. Upon electroreduction the rms roughness value increased from 1.1 nm to 1.5 nm for a 1 × 1 μm^2 scan (ESI,† Fig. A2).

The electrochemical activity of the azo groups is thought to depend strongly on the layer structure and density. Previous studies of self-assembled monolayers of azobenzenethiols on gold[28] and nitroazobenzene films on carbon[18] suggest that densely packed layers severely inhibit the ion penetration into the layers and, in turn, reduce the accessibility of the azo groups, making them less electro-active. Our work on azobenzenes on Si and a recent study of Jung *et al.*[21] on azobenzenethiols on gold show the possibility of electrochemical cleavage of azo groups that are present in films, most likely due to a lower layer packing.

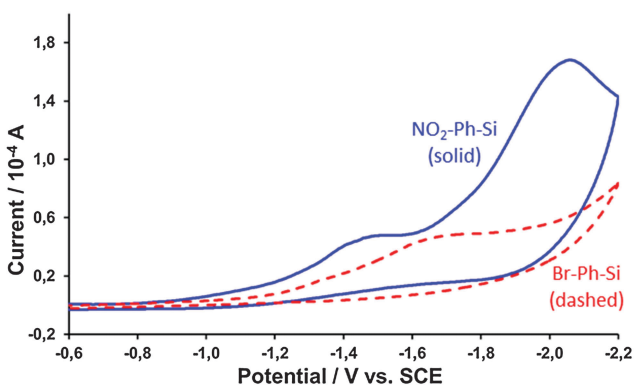

Fig. 3 Electroreduction of electrografted layers on silicon (111) prepared from 4-NBD (blue solid) and 4-BBD (red dashed).

By comparing the surface areas of the peaks in Fig. 3 one can estimate the percentage of the azo-bond formation. The ratio between the surface area of the peak of the NO_2 to NH_2 reduction and the one of the azo-bond cleavage is ∼7. Taking into account that the azo-bond and nitro reduction require 4 and 6 electrons,[20,29] respectively, the extent of azo-bond formation is 22%, assuming that both reduction processes are complete. This number is similar to the one obtained by the XPS results on 4-BBD, showing that 24% of the bromobenzene is attached *via* an azo bond.

Electrografted Si samples that were exposed to subsequent reduction cycles to reduce the nitro and azo groups were also analyzed by XPS. Fig. 4a shows the typical Br_{3d} region spectra of 4-BBD-modified silicon samples. Upon reduction down to −2.2 V the intensity of the Br_{3d} XPS peak decreases, which indicates that Br-substituted aryl derivatives are released from the surface. The average degree of Br reduction was found to be 43% (ESI,† Fig. A3). This decrease is attributed to the azo-bond reduction in the thin films of 4-BBD-modified Si samples.

While only ∼25% of the linkages are azo bonds, up to 40% of the material is lost upon the electrochemical reduction. This may indicate that—on average—the azo bonds are closer to the surface than the biphenyl bonds. Another peculiar observation is that the 40% loss of the layer material results in a layer thickness reduction of only ∼25%. Presumably the layer is rather rigid as for fluid materials the layer thickness would be proportional to the amount of deposited material as the layer is expected to collapse in that case.

The XPS results of 4-NBD-modified samples are presented in Fig. 4b. As discussed in Section 3.1 the peak near 406 eV is attributed to the nitro group and the 400 eV peak is attributed to the azo and amino groups. For the electrografted nitrobenzene that was not further reduced (Fig. 4b, red) the N_{1s} peak ratio of 406 eV/400 eV was found to be ∼0.72. During the CV cycle down to −2.2 V (Fig. 4b, orange) we expect both reductions, *i.e.* azo to amino and nitro to amino, to happen. After this cycle the 406 eV/400 eV ratio was found to be ∼0.09. The decrease of the NO_2 peak is a signal for the loss of the NO_2-substituted aryl derivatives like in the case of 4-BBD-modified Si and also an indication for the transformation of the nitro group. The NO_2 signal does not disappear completely. Apparently a small amount of these groups—which may be connected to the surface *via* biphenyl coupling (Scheme 1, box I)—is not easily reduced.

Fig. 4b also shows the results of the electroreduction of the 4-NBD-modified Si in the range between −0.6 and −1.5 V *vs.* SCE (blue), thus only the reduction of the azo units and no reduction of the nitro groups. First it is noted that the intensity of the 406 eV (NO_2) peak is higher compared to the one obtained after the reduction in the range between

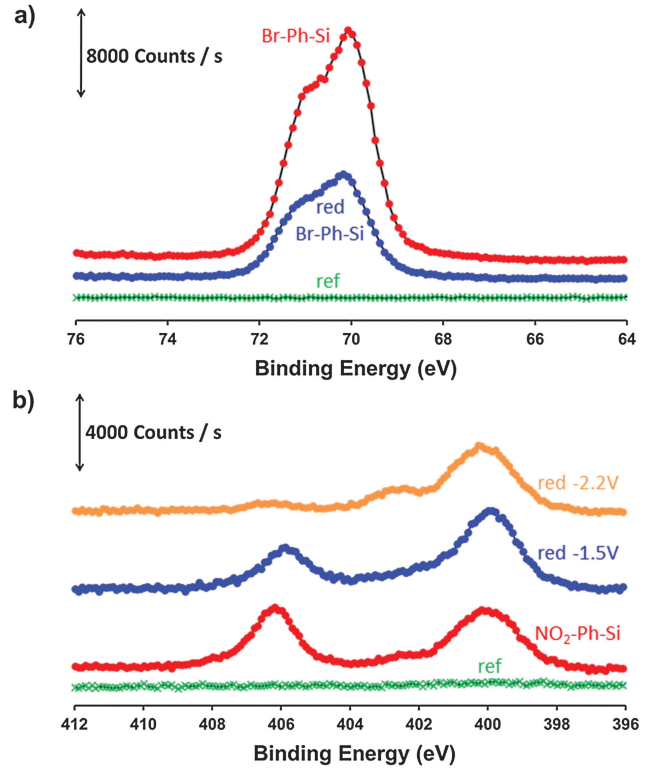

Fig. 4 (a) Br_{3d} region spectra of 4-BBD-modified Si (red) and after the reduction down to −2.2 V (blue). The spectrum of the unmodified surface is also given (ref, green), (b) N_{1s} region spectra of the unmodified surface (ref, green), 4-NBD-modified Si (red), after the reduction down to −1.5 V (blue) and −2.2 V (orange).

−0.6 and −2.2 eV *vs.* SCE. The peak ratio of 406 eV/400 eV in this case was found to be ∼0.47 (Fig. 4b, blue). This value is in between the results obtained for the non-reduced and fully reduced 4-NBD-modified Si surface. Some of the originally present NO_2 groups that were connected to the surface *via* the azo bond are lost upon the reduction to −1.5 V. As shown by the XPS data the grafted layer still does contain NO_2 groups, which have not been reduced yet to amines. This is because the potential for the NO_2 to NH_2 reduction (*i.e.* −2.1 V) was not applied yet. In acetonitrile the two processes, the reduction of azo bonds and the nitro to amino conversion, can be separated. This confirms the earlier proposition that the two different types of reduction take place at different voltages.

Electrochemical analysis and XPS show that the reduction of nitro to amino groups and the azo cleavage can also occur in aprotic media such as ACN. These processes can only take place in the presence of protons. This may be explained by small amounts of water, possibly present in the ACN as well as in the hydration layer of the grafted layers, which is sufficient to supply this demand for protons.

3.3 Functionalization of the reduced layers

The reduced layers were functionalized by reaction with TFAA, yielding amides. Fig. 5 summarizes typical XPS data on the TFAA modification of different samples. In Fig. 5a we compare three samples treated with TFAA: 4-NBD- and 4-BBD-modified Si samples—which were further reduced in a voltage range of −0.6 to −2.2 V *vs.* SCE (red and blue, respectively)—and as a reference sample, 4-BBD-modified Si that was not further electroreduced (green). The F_{1s} region spectra show significantly larger amounts of organic fluorine at 688 eV for the electroreduced samples treated with TFAA (red and blue circles) compared to the reference sample, which shows a peak at 686 eV (green). The last peak can be attributed to inorganic fluorine and indicated the presence of the tetrafluoroborate ion (BF_4^-) used in the procedure. In the red and blue plots this peak appears as a shoulder of the larger peak at 688 eV. The successful amide formation can also be seen by closely examining the C_{1s} region spectrum (Fig. 5b), since carbon bound to elements with increased electronegativity like fluorine will give signals at increased binding energies. In more detail, the C_{1s} region of the electroreduced 4-NBD Si sample treated with TFAA shows two C_{1s} peaks at high bonding energies referred to as $\underline{C}$–F_3 and ($\underline{C}$═O)CF_3 (Fig. 5b, peaks D and C, respectively).[30] It is noticed that the ratio of the these two peak

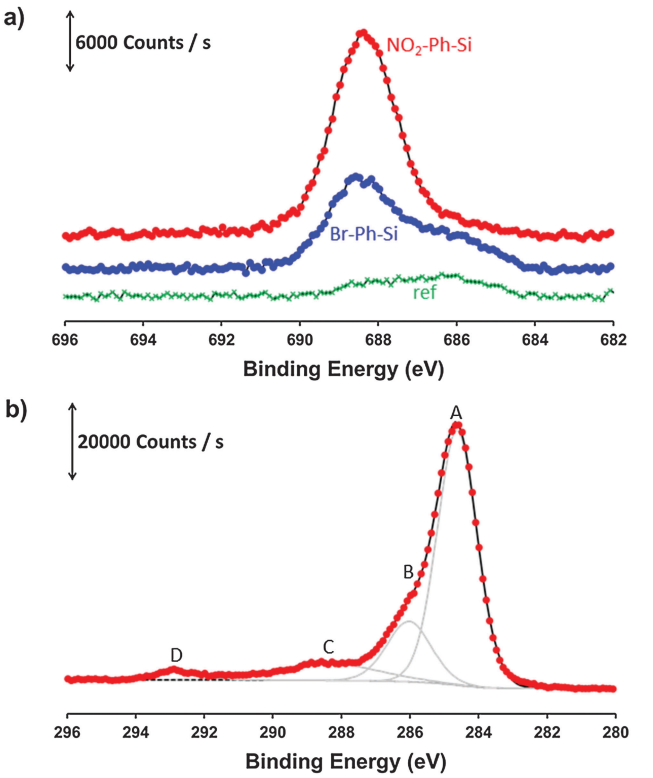

Fig. 5 (a) F_{1s} region spectra of electrografted and electroreduced nitrobenzene (red) and bromobenzene (blue) on Si samples (down to −2.2 V) and a bromobenzene electrografted, but not reduced Si sample (ref, green, down to −0.6 V). All samples were treated with TFAA; (b) C_{1s} region spectrum of an electrografted nitrobenzene on a Si sample down to −2.2 V, followed by the treatment with TFAA. Peak A refers to $\underline{C}$–H/$\underline{C}$–C, B to $\underline{C}$–N, C to ($\underline{C}$═O)CF_3 and peak D to $\underline{C}$–F_3. The dashed line represents the baseline, the deconvoluted peaks are given in grey solid lines and the black solid line represents the envelop.

areas is not 1:1, which we contribute to small amounts of sample contamination before any aryldiazonium treatment (data not shown).

The presence of a certain amount of TFA groups on the treated 4-BBD-modified Si sample can be rationalized by formation of amino groups as a result of the azo-bond electroreduction at voltages around −1.5 V *vs.* SCE. Since both the nitro and azo groups were reduced to amines in the case of 4-NBD-modified samples (Scheme 1, steps c and d), the amount of amino groups per attached aryl derivative is higher as compared to 4-BBD-modified samples, which is also observed by XPS as presented in Fig. 5a.

4 Conclusions

The diazonium salts 4-NBD and 4-BBD were electrografted onto H-terminated Si(111) at voltages of −0.18 and −0.52 V *vs.* SCE, respectively. The electrografting reaction is not specific, *i.e.* only forming Si–C bonds, and does not stop at the monolayer coverage. Instead, layers of 2–7 nm thickness are obtained. The layer thickness increases with an increase in reaction time, but hardly with an increase in aryldiazonium concentration. For both diazonium salts it was concluded that 22–24% of the aryl moieties are connected to the surface by azo-linkers. Electroreduction at potentials that were more negative than the grafting potential reduced the azo units to amino groups. The required potentials were −1.5 and −1.65 V *vs.* SCE for 4-NBD and 4-BBD-modified Si, respectively. The reduction of the azo bonds leads to slightly thinner layers, due to scission. Monolayers, however, are not obtained due to the presence of the biphenyl bonds that are not susceptible to electroreduction. The nitro groups present in 4-NBD-modified Si have been reduced to amino groups at about −2.1 V *vs.* SCE. Since the azo groups can be reduced to amino groups, it is concluded that amino-functionalized surfaces can be obtained from electrografting of non-nitro containing aryldiazonium ions. The presence of reactive amino functionalities after electroreduction of the azo units was proven by the formation of amide bonds by reaction with TFAA.

Our research demonstrates that multifunctional organic layers on Si surfaces can be formed by a straightforward and well-controlled electrochemical process. When applied to silicon nanowires that are part of multi-array devices, amino functionalities can be formed and functionalized individually. This would result in easy fabrication of arrays with different functionalities on the individual nanowires. In the case of BBD, multifunctionality on a single nanowire can be achieved. The aryl bromine can participate in reactions such as Suzuki or Sonogashira coupling, while the azo-derived amino functionality can be used in the formation of imines or amides.

Current research in our laboratory is directed towards the implementation of the described electrochemistry for the independent modification of SiNWs that are part of an array sensor platform.

Acknowledgements

The Dutch Technology Foundation STW is acknowledged for financial support (project number: 10255). We thank Dr Liza Rassaei (Delft University of Technology) for stimulating discussions.

References

1 M. Dufva, *Biomol. Eng.*, 2005, **22**, 173–184.
2 M. J. E. Fischer, in *Surface Plasmon Resonance*, ed. N. J. de Mol, Humana Press, 1st edn, 2010, ch. 55–73, vol. 627.
3 F. Patolsky, G. F. Zheng and C. M. Lieber, *Anal. Chem.*, 2006, **78**, 4260–4269.
4 E. Stern, A. Vacic and M. A. Reed, *IEEE Trans. Electron Devices*, 2008, **55**, 3119–3130.
5 Y. L. Bunimovich, Y. S. Shin, W. S. Yeo, M. Amori, G. Kwong and J. R. Heath, *J. Am. Chem. Soc.*, 2006, **128**, 16323–16331.
6 L. C. P. M. de Smet, D. Ullien, M. Mescher and E. J. R. Sudhölter, in *Nanowires – Implementations and Applications*, ed. A. Hashim, InTech, 2011.
7 E. J. Faber, L. C. P. M. de Smet, W. Olthuis, H. Zuilhof, E. J. R. Sudholter, P. Bergveld and A. van den Berg, *ChemPhysChem*, 2005, **6**, 2153–2166.
8 R. Hunger, W. Jaegermann, A. Merson, Y. Shapira, C. Pettenkofer and J. Rappich, *J. Phys. Chem. B*, 2006, **110**, 15432–15441.
9 M. A. Mohd Azmi, Z. Tehrani, R. P. Lewis, K.-A. D. Walker, D. R. Jones, D. R. Daniels, S. H. Doak and O. J. Guy, *Biosens. Bioelectron.*, 2014, **52**, 215–224.
10 J. Yun, C. Y. Jin, J. H. Ahn, S. Jeon and I. Park, *Nanoscale*, 2013, **5**, 6851–6856.
11 F. Effenberger, G. Gotz, B. Bidlingmaier and M. Wezstein, *Angew. Chem., Int. Ed.*, 1998, **37**, 2462–2464.
12 M. Delamar, R. Hitmi, J. Pinson and J. M. Saveant, *J. Am. Chem. Soc.*, 1992, **114**, 5883–5884.
13 M. Couture, S. S. Zhao and J.-F. Masson, *Phys. Chem. Chem. Phys.*, 2013, **15**, 11190–11216.
14 C. H. de Villeneuve, J. Pinson, M. C. Bernard and P. Allongue, *J. Phys. Chem. B*, 1997, **101**, 2415–2420.
15 J. Pinson and F. Podvorica, *Chem. Soc. Rev.*, 2005, **34**, 429–439.
16 A. Shabani, A. W. H. Mak, I. Gerges, L. A. Cuccia and M. F. Lawrence, *Talanta*, 2006, **70**, 615–623.
17 P. Allongue, C. H. de Villeneuve, G. Cherouvrier, R. Cortes and M. C. Bernard, *J. Electroanal. Chem.*, 2003, **550**, 161–174.
18 P. A. Brooksby and A. J. Downard, *J. Phys. Chem. B*, 2005, **109**, 8791–8798.
19 P. Doppelt, G. Hallais, J. Pinson, F. Podvorica and S. Verneyre, *Chem. Mater.*, 2007, **19**, 4570–4575.
20 S. S. C. Yu, E. S. Q. Tan, R. T. Jane and A. J. Downard, *Langmuir*, 2007, **23**, 11074–11082.
21 H. J. Jung, H. Min, H. Yu, T. G. Lee and T. D. Chung, *Chem. Commun.*, 2010, **46**, 3863–3865.

22 C. M. Herzinger, B. Johs, W. A. McGahan, J. A. Woollam and W. Paulson, *J. Appl. Phys.*, 1998, **83**, 3323–3336.
23 P. Finn and W. L. Jolly, *Inorg. Chem.*, 1972, **11**, 1434–1435.
24 K. E. Lee, M. A. Gomez, T. Regier, Y. F. Hu and G. P. Demopoulos, *J. Phys. Chem. C*, 2011, **115**, 5692–5707.
25 M. Toupin and D. Belanger, *J. Phys. Chem. C*, 2007, **111**, 5394–5401.
26 J. Lyskawa, A. Grondein and D. Belanger, *Carbon*, 2010, **48**, 1271–1278.
27 K. Roodenko, M. Gensch, J. Rappich, K. Hinrichs, N. Esser and R. Hunger, *J. Phys. Chem. B*, 2007, **111**, 7541–7549.
28 D. J. Campbell, B. R. Herr, J. C. Hulteen, R. P. VanDuyne and C. A. Mirkin, *J. Am. Chem. Soc.*, 1996, **118**, 10211–10219.
29 P. Allongue, M. Delamar, B. Desbat, O. Fagebaume, R. Hitmi, J. Pinson and J. M. Saveant, *J. Am. Chem. Soc.*, 1997, **119**, 201–207.
30 F. Pippig, S. Sarghini, A. Hollander, S. Paulussen and H. Terryn, *Surf. Interface Anal.*, 2009, **41**, 421–429.